

This is a copy of the published version, or version of record, available on the publisher's website. This version does not track changes, errata, or withdrawals on the publisher's site.

# The Ariel payload design post-PDR

Paul Eccleston, Andrew Caldwell, Georgia Bishop, Lucile Desjonquieres, Rachel Drummond, Alex Davidson, Martin Whalley, Martin Caldwell, Chris Pearson, Caroline Simpson, Sandy Fok, Davide Bruzzi, Alex Davies, Mark Anderson, Pranav Umesh, Enzo Pascale, Gianluca Morgante, Mauro Focardi, Giorgio Savini, Marc Ollivier, Mirosław Rataj, Giuseppe Malaguti, Giovanna Tinetti, Andrea Tozzi, Paolo Chioetto, Emanuele Pace, Paola Zuppella, Giampaolo Preti, Christophe Serre, Jose M. Gomez, Gustavo Alonso, Javier Perez, Neil Bowles, Keith Nowicki, Jérôme Martignac, Michel Berthé, Pascale Danto, Martin Crook, Matthew Hills, Charles Padley, Semu Makinen, Zsolt Kovacs, Janos Szoke, Peter Szirovicza, Mateusz Sobiecki, Konrad Skup, Piotr Wawer, Roland Ottensamer, Warren Holmes, Renaud Goullioud, Markus Czupalla, Niels Christian Jessen, Soren Pedersen, Tom Ray, Deirdre Coffey, Lukas Steiger, Carlos Compostizo, Ricardo Machado, Andrea Bocchieri, Lorenzo Mugnai, Stephan Birkmann, Salma Fahmy, Ludovic Puig, Delphine Jollet, Anders Svedevall, Thierry Tirolien, Jean-Christophe Salvignol, Jean-Philippe Halain

## Published version information:

**Citation:** Paul Eccleston et al., The Ariel payload design post-PDR, Proceedings Volume 13092, Proceedings Volume 13092, Space Telescopes and Instrumentation 2024: Optical, Infrared, and Millimeter Wave; 130921B (2024)

**DOI:** <https://doi.org/10.1117/12.3019713>

Copyright 2024 Society of Photo-Optical Instrumentation Engineers (SPIE). One print or electronic copy may be made for personal use only. Systematic reproduction and distribution, duplication of any material in this publication for a fee or for commercial purposes, and modification of the contents of the publication are prohibited.

This version is made available in accordance with publisher policies. Please cite only the published version using the reference above. This is the citation assigned by the publisher at the time of issuing the APV. Please check the publisher's website for any updates.

This item was retrieved from **ePubs**, the Open Access archive of the Science and Technology Facilities Council, UK. Please contact [epublications@stfc.ac.uk](mailto:epublications@stfc.ac.uk) or go to <http://epubs.stfc.ac.uk/> for further information and policies.

# The Ariel Payload Design post-PDR

Paul Eccleston <sup>\*a</sup>, Andrew Caldwell <sup>a</sup>, Georgia Bishop <sup>a</sup>, Lucile Desjonquieres <sup>a</sup>, Rachel Drummond <sup>a</sup>, Alex Davidson <sup>a</sup>, Martin Whalley <sup>a</sup>, Martin Caldwell <sup>a</sup>, Chris Pearson <sup>a</sup>, Caroline Simpson <sup>a</sup>, Sandy Fok <sup>a</sup>, Davide Bruzzi <sup>a</sup>, Alex Davies <sup>a</sup>, Mark Anderson <sup>a</sup>, Pranav Umesh <sup>a</sup>, Enzo Pascale <sup>b</sup>, Gianluca Morgante <sup>c</sup>, Mauro Focardi <sup>d</sup>, Giorgio Savini <sup>e</sup>, Marc Ollivier <sup>f</sup>, Mirosław Rataj <sup>h</sup>, Giuseppe Malaguti <sup>c</sup>, Giovanna Tinetti <sup>e</sup>, Andrea Tozzi <sup>d</sup>, Paolo Chioetto <sup>g</sup>, Emanuele Pace <sup>j</sup>, Paola Zuppella <sup>g</sup>, Giampaolo Preti <sup>j</sup>, Christophe Serre <sup>k</sup>, Jose M Gomez <sup>k</sup>, Gustavo Alonso <sup>l</sup>, Javier Pérez <sup>l</sup>, Neil Bowles <sup>m</sup>, Keith Nowicki <sup>m</sup>, Jerome Martignac <sup>n</sup>, Michel Berthe <sup>n</sup>, Pascale Danto <sup>cc</sup>, Martin Crook <sup>p</sup>, Matthew Hills <sup>p</sup>, Charles Padley <sup>p</sup>, Semu Makinen <sup>q</sup>, Zsolt Kovacs <sup>r</sup>, Janos Szoke <sup>r</sup>, Peter Szivovics <sup>r</sup>, Mateusz Sobiecki <sup>h</sup>, Konrad Skup <sup>h</sup>, Piotr Wawer <sup>h</sup>, Roland Ottensamer <sup>s</sup>, Warren Holmes <sup>t</sup>, Renaud Goullioud <sup>t</sup>, Markus Czupalla <sup>x</sup>, Niels Christian Jessen <sup>u</sup>, Soren Pedersen <sup>u</sup>, Tom Ray <sup>v</sup>, Deirdre Coffey <sup>ee</sup>, Lukas Steiger <sup>w</sup>, Carlos Compostizo <sup>aa</sup>, Ricardo Machado <sup>bb</sup>, Andrea Bocchieri <sup>b</sup>, Lorenzo Mugnai <sup>dd</sup>, Stephan Birkmann <sup>y</sup>, Salma Fahmy <sup>z</sup>, Ludovic Puig <sup>z</sup>, Delphine Jollet <sup>z</sup>, Anders Svedevall <sup>z</sup>, Thierry Tirolien <sup>z</sup>, Jean-Christophe Salvignol <sup>z</sup>, Jean-Philippe Halain <sup>z</sup>

<sup>a</sup> RAL Space, STFC – Rutherford Appleton Laboratory, Harwell Campus, Didcot, OX11 0QX, UK;

<sup>b</sup> Sapienza Università di Roma, Dept of Physics, Rome, Italy;

<sup>c</sup> INAF - Osservatorio di Astrofisica e Scienza dello spazio di Bologna, Via Piero Gobetti 93/3, 40129 Bologna, Italy;

<sup>d</sup> INAF - OAA Arcetri Astrophysical Observatory, Largo E. Fermi 5, 50125 Firenze, Italy

<sup>e</sup> University College London, Gower Street, London, WC1E 6BT, UK;

<sup>f</sup> IAS, Université de Paris-Sud, CNRS UMR 8617, Orsay F-91405, France;

<sup>g</sup> CNR-IFN Padova, Via Trasea 7, 35131 Padova, Italy;

<sup>h</sup> Space Research Centre Polish Academy of Sciences, Bartycka 18A, 00-716 Warsaw, Poland;

<sup>j</sup> University of Florence, Via Sansone, 1, 50019 Sesto Fiorentino (FI), Florence, Italy;

<sup>k</sup> Institut de Ciències de l'Espai, (CSIC-IEEC), Campus UAB, 08193 Bellaterra, Barcelona, Spain;

<sup>l</sup> Instituto Universitario de Microgravedad “Ignacio Da Riva” (IDR/UPM), Universidad Politécnica de Madrid, Plaza del Cardenal Cisneros 3, 28040 Madrid, Spain;

<sup>m</sup> University of Oxford, Clarendon Laboratory, Parks Road, Oxford OX1 3PU, UK;

<sup>n</sup> Université Paris-Saclay, Université Paris Cité, CEA, CNRS, AIM, 91191, Gif-sur-Yvette, France;

<sup>p</sup> Technology Department, STFC – Rutherford Appleton Laboratory, Harwell Campus, Didcot, OX11 0QX, UK;

<sup>q</sup> OHB System AG, Manfred-Fuchs-Str. 1, D-82234 Weßling, Germany;

<sup>r</sup> Admatis Ltd, 5 Kando Kalman Str, 3534 Miskolc, Hungary;

<sup>s</sup> Institut fuer Astrophysik der Universitaet Wien, Sternwartestrasse 77, A-1180 Wien, Austria;

<sup>t</sup> Jet Propulsion Laboratory (JPL), California Institute of Technology, Pasadena, CA 91009, USA;

<sup>u</sup> Elektrovej, Building 328, 2800 Kgs Lyngby, Denmark Technical University (DTU), Copenhagen, Denmark;

<sup>v</sup> Dublin Institute for Advanced Studies, 31 Fitzwilliam Place, Dublin 2, Ireland;

<sup>w</sup> TOPTEC, Institute of Plasma Physics of the Czech Academy of Sciences, Za Slovankou 3, 182 00 Prague, Czechia;

<sup>x</sup> FH Aachen University of Applied Sciences, Hohenstaufenallee 6, 52064 Aachen, Germany;

<sup>y</sup> ESA ESAC, European Space Astronomy Centre, Camino Bajo del Castillo s/n, 28692 Villanueva de la Cañada, Madrid, Spain;

<sup>z</sup> ESA ESTEC, Keplerlaan 1, NL-2201 AZ Noordwijk, The Netherlands;

<sup>aa</sup> SENER Aeroespacial S.A, Avda. de Zugazarte, 56, 48930 Getxo, Bizkaia, Bilbao, Spain

<sup>bb</sup> Active Space Technologies (AST), Parque Industrial de Taveiro, Lote 12, 3045-508 Coimbra, Portugal

<sup>cc</sup> Centre National d'Etudes Spatiales (CNES), 18 avenue Edouard Belin 31401 Toulouse Cedex 9, France

<sup>dd</sup> Cardiff University, Queens Buildings, The Parade, Cardiff, CF24 3AA, UK.

<sup>ee</sup> University College Dublin, Belfield, Dublin 4, Ireland

\*Corresponding Author: [paul.eccleston@stfc.ac.uk](mailto:paul.eccleston@stfc.ac.uk); phone: +44 1235 446366;

## ABSTRACT

The Ariel space mission will characterize spectroscopically the atmospheres of a large and diverse sample of hundreds of exoplanets. Through the study of targets with a wide range of planetary parameters (mass, density, equilibrium temperature) and host star types the origin for the diversity observed in known exoplanets will be better understood. Ariel is an ESA Medium class science mission (M4) with a spacecraft bus developed by industry under contract to ESA, and a Payload provided by a consortium of national funding agencies in ESA member states, plus contributions from NASA, the CSA and JAXA.

The payload is based on a 1-meter class telescope operated at below 60K, built all in Aluminium, which feeds two science instruments. A multi-channel photometer and low-resolution spectrometer instrument (the FGS, Fine Guidance System instrument) operating from 0.5 – 1.95 microns in wavelength provides both guidance information for stabilizing the spacecraft pointing as well as vital scientific information from spectroscopy in the near-infrared and photometry in the visible channels. The Ariel InfraRed Spectrometer (AIRS) instrument provides medium resolution spectroscopy from 1.95 – 7.8 microns wavelength coverage over two instrument channels. Supporting subsystems provide the necessary mechanical, thermal and electronics support to the cryogenic payload.

This paper presents the overall picture of the payload for the Ariel mission. The payload tightly integrates the design and analysis of the various payload elements (including for example the integrated STOP analysis of the Telescope and Common Optics) in order to allow the exacting photometric stability requirements for the mission to be met. The Ariel payload has passed through the Preliminary Design Review (completed in Q2 2023) and is now developing and building prototype models of the Telescope, Instruments and Subsystems (details of which will be provided in other contributions to this conference). This paper will present the current status of the development work and outline the future plans to complete the build and verification of the integrated payload.

**Keywords:** Astronomy, Instrumentation, Exoplanets, Spectroscopy, Space, Transit, Telescope, Atmosphere

## 1. INTRODUCTION

Ariel, the atmospheric remote-sensing infrared exoplanet large-survey, is the fourth medium class mission within ESA's Cosmic Vision science programme. Ariel is the first mission dedicated to studying the atmospheres of a statistically large and diverse sample of transiting exoplanets ( $\geq 500$ ) through a combination of transit photometry and spectroscopy. Ariel aims to measure the chemical composition and thermal structures of exoplanets extending from gas giants (Jupiter or Neptune like) to super-Earths, that (currently) orbit in the very hot to warm zones of their F to M-type host stars, opening up the way to large-scale, comparative planetology and allowing to address the following fundamental questions:

- What are the physical processes shaping planetary atmospheres?
- What are exoplanets made of?
- How do planets and planetary systems form and evolve?

Ariel is due for launch in 2029 on board an Ariane 6.2 in a dual launch configuration with the Comet Interceptor mission. It will operate from an orbit around the second Lagrange point of the Sun-Earth system (L2), which offers the benefit of a stable thermal environment thanks to the constrained relative orientation of the Sun and Earth to the spacecraft. The nominal mission lifetime is 4 years, however the mission will be sized to allow a lifetime extension to 6 years.

### **Mission & Spacecraft Overview**

The spacecraft is composed of the Service Module (SVM), onto which the Payload Module (PLM) is integrated. The SVM hosts all the platform elements of the spacecraft such as the attitude and orbit control, power, data handling and communications systems, as well as warm electronics units and the cryocooler of the payload. The PLM hosts the telescope and detection chain of the payload, along with so-called “V-groove” structures, which serve to thermally decouple the PLM from the SVM. The S/C will be three-axis stabilized and oriented such that the PLM is maintained in the shadow of the SVM, enabling the telescope assembly to cool passively, reaching an operating temperature <70 K. The total spacecraft wet mass is approximately 1410kg with a power budget of 1kW.

The PLM holds the telescope assembly, containing an afocal off-axis Cassegrain telescope and common optics, which direct the incoming light to the two science instruments. The instruments consist of the Ariel IR Spectrometer (AIRS), providing spectroscopy over the wavelength range 1.95 - 7.80  $\mu\text{m}$  and the Fine Guidance System (FGS) instrument which contains 3 photometric channels, VISPhot (0.50-0.60  $\mu\text{m}$ ); FGS1 (0.60-0.80  $\mu\text{m}$ ) and FGS2 (0.80-1.10  $\mu\text{m}$ ), as well as a low-resolution spectrometer covering the waveband 1.10-1.95  $\mu\text{m}$ . The FGS1 and FGS2 channels also serve as a Fine Guidance Sensor in the attitude control loop of the spacecraft, allowing to achieve the pointing stability required to meet the science objectives.

The overall responsibility for the mission lies with ESA, with the Ariel Mission Consortium (AMC) being responsible for the PLM and warm payload units as well as for the IOSDC. The members of the AMC are nationally funded by their respective national agencies and the overall collaboration is governed by a Multi-Lateral Agreement (MLA) to which all agencies are signatories.

Further details of the mission and spacecraft SVM design can be found in Salvignol et al [1].

## **2. PAYLOAD SYSTEM DESIGN AND ARCHITECTURE**

The integrated payload comprises an off-axis Cassegrain telescope made entirely of aluminum, directing a collimated beam into two distinct instrument modules. Operating in the visible to infrared, the Fine Guidance System (FGS) features three photometry channels spanning from 0.50  $\mu\text{m}$  to 1.1  $\mu\text{m}$ . Among these channels, two serve as a redundant system, ensuring guidance and closed-loop control for the AOCS. Additionally, this module houses a low-resolution spectrometer (R = ~15) operating within the 1.1  $\mu\text{m}$  – 1.95  $\mu\text{m}$  waveband.

A second instrument module, named the Ariel IR Spectrometer (AIRS), offers spectral resolutions ranging from 30 to 100 across a waveband from 1.95  $\mu\text{m}$  to 7.8  $\mu\text{m}$ . To maintain operational temperatures, the payload module employs passive cooling techniques, reaching approximately 55 K through isolation from the spacecraft bus, facilitated by V-Groove radiators and isolating Bipods. The only components requiring active cooling are the detectors for the AIRS instrument, which are cooled to below 42 K using an active Ne JT cooler. The design of the payload and its associated instruments is depicted below.

The major items, as shown in Figure 2-1, Figure 2-2 and Figure 2-3 are:

- **Cold PLM:**
  - The Telescope Assembly (TA) is based on an optical off-axis Cassegrain telescope system that consists of the Telescope Optical Bench (TOB) and the Metering Structure (TMS), of the primary mirror M1, secondary mirror at prime focus M2 with a re-focusing mechanism on the M2 mirror (M2M), the M3 and M4 beams to collimate the beam and direct it towards the optical bench, and of the TA Baffle.
  - A set of common optics to split the incoming beam between the AIRS and FGS instruments including the M5 mirror to direct the incoming beam, the dichroics to split the FGS and spectrometer light, and formatting optics to inject the light into the spectrometer correctly.

- The Ariel IR Spectrometer (AIRS) to use the light focused by the telescope to perform the high resolution spectroscopy extended into the far infrared, including all optics and structure plus detectors, cold front-end electronics (cFEE), and interface to the AIRS DCU.
- Fine Guidance Sensor / Visible Photometer / Near-IR Spectrometer (FGS/VISPhot/NIRSpec), including all optics and dichroics to split into the 4 separate channels, prime and redundant detectors and cold front end electronics (cFEE).
- Thermal hardware: active cooler cold head for Neon JT cooler, passive radiator for cooling of FGS detectors and cFEEs, V-grooves and Bipods to isolate the cold PLM from the warmer SVM.
- **Warm SVM mounted units:**
  - Instrument Control Unit (ICU) housing the central data processing unit (DPU) for the spectrometer data, a power supply unit (PSU), communication and interface to the A-DCU and TCU, and a Commanding and Data Processing Unit (CDPU).
  - AIRS Detector Control Unit (A-DCU) which includes a power and data interface to the ICU, housekeeping & central logic, biasing, data acquisition & pre-processing for the spectrometer and thermal control and monitoring for AIRS.
  - Telescope Control Unit (TCU) providing power and data interface to the ICU, power distribution & central logic, M2M mechanism control, and thermal monitoring and control of the telescope.
  - FGS Control Unit (FCU) electronics incorporating the FGS/VISPhot/NIRSpec wFEE, the control and processing electronics and software for determining the pointing from the FGS data and transmitting this information to the spacecraft.
  - Active Cooler System (ACS):
    - Cooler Control Electronics (CCE), including power and conditioned signals to the cooler compressor, monitoring of cooler housekeeping data, and stabilization of cold head temperatures (if necessary).
    - Cooler ComPressors Assembly (CPA)
    - Cooler gas handling panel incorporating fill connections, filtering etc., the Cooler Ancillary Panel (CAP)

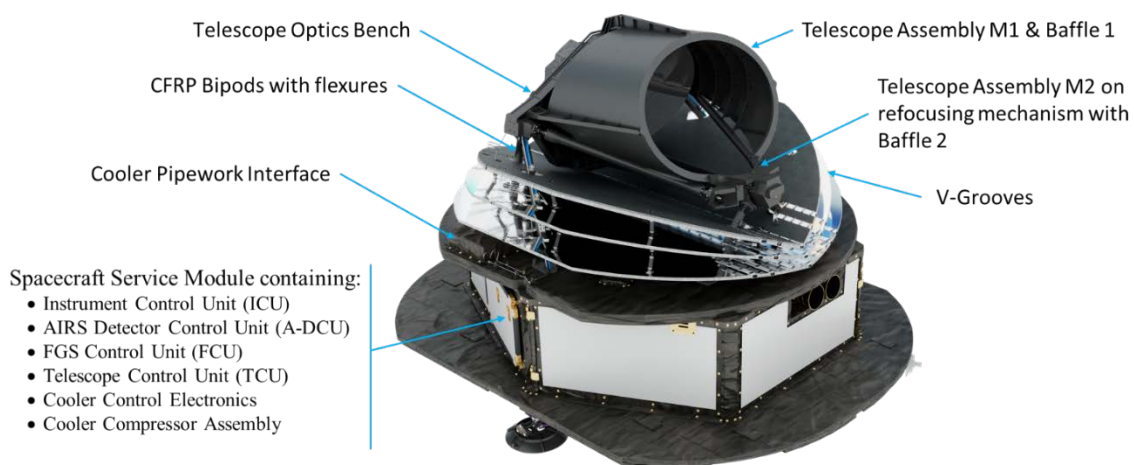


Figure 2-1: Illustration of the Ariel PLM and SVM



Figure 2-2: Illustration of the rear of the Ariel PLM

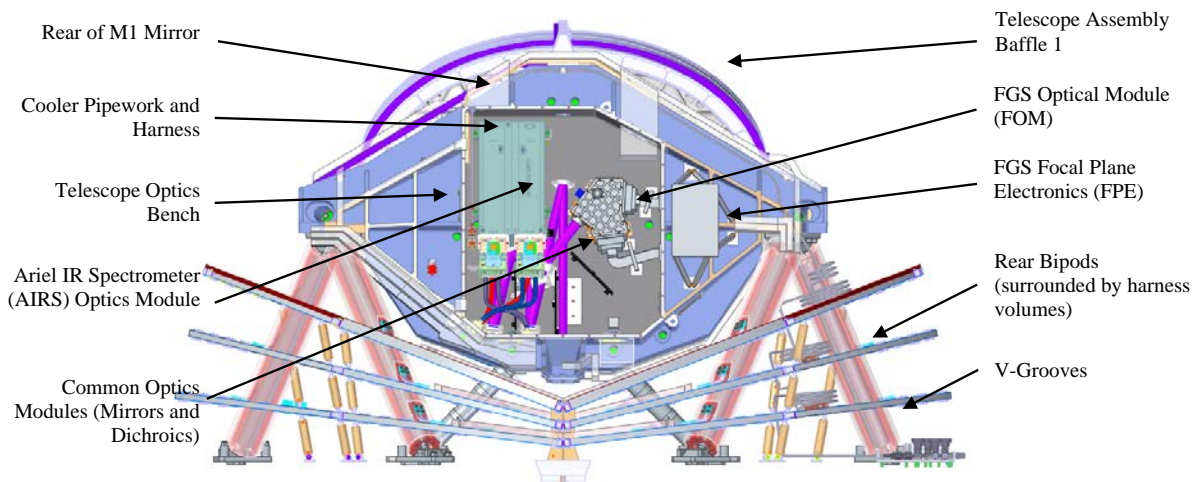


Figure 2-3: Illustration of the accommodation on the Ariel PLM Optical Bench

### Responsibilities and Modularity

The baseline design architecture has been selected to maintain a high degree of modularity in the design. This helps both technically and programmatically in allowing independent development of the instrument / module / subsystem designs and in giving the maximum flexibility for future changes. To this end the optical design of the modules are largely decoupled from one another by the selection of either a collimated (nominally) aberration free beam or a focus as the interface between modules.

A common optical bench (TOB) (separate from the structures of the individual modules and the telescope primary mirror) has been selected as the design baseline. The assumption of responsibility for the TOB by the consortium team allows the instruments and telescope to be built, assembled, aligned and tested as a unit and pre-calibrated prior to delivery to ESA. The co-alignment of the modules (critical to the success of the mission due to the shared field of view) can then be assured and checked at the earliest possible stage.

While the consortium contains many 17 different ESA member state countries that contribute to the work, the hardware provision is focused in a smaller number. The Consortium has distributed effort according to the skills and resources in the participating institutes and reflecting the areas of national interest in the science of Ariel. This also ensures that a broad spectrum of state-of-the-art and appropriate technical design expertise is brought to bear on the design,

construction and test of the instrument. An overview of the division of work between the participating countries is shown in Figure 2-4 below, further details of the management techniques used to coordinate this large consortium can be found in Eccleston et al [2].

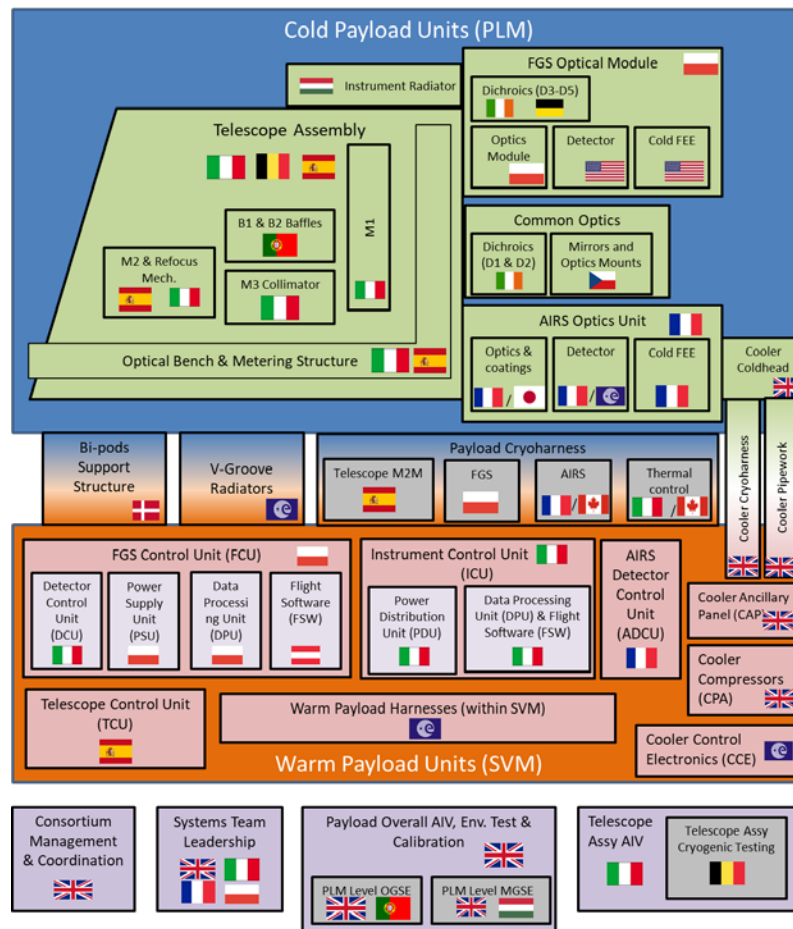


Figure 2-4: Overview of National Responsibilities

### Design philosophy

The design baseline is that all of the cryogenic components of the payload architecture are manufactured from a common material, aluminium 6061 T651 or T652 (or 6082 T651) alloy. This ensures that the design has a matched CTE, allowing warm alignment of the payload to proceed, with a high degree of confidence that this will be maintained when cooled to operating temperatures. All-reflective optical elements in the design are also assumed to be manufactured from aluminium for the same reason. This builds on the significant design heritage within Europe of building all aluminium space instruments for cryogenic operation such as Herschel SPIRE & PACS and JWST MIRI. Building in aluminium also provides a robust design approach with minimum technical risk (and straight-forward options for rework if and when this becomes necessary during AIV activities, unlike with other options such as SiC).

### Noise budget and design for optimum performance

Ariel's orbit around the Sun-Earth Lagrange point L2 provides a thermally (and therefore photometrically) stable environment for the telescope and instruments. The mission's primary requirement is to achieve sufficient photometric stability to measure atmospheric signals with a precision of 10-100 ppm relative to the stellar flux over timescales relevant to transit and eclipse observations.

The design of the Ariel payload incorporates lessons learned from previous exoplanetary atmosphere measurements conducted by missions such as Spitzer and HST, as well as from ground-based instruments. Key features enabling Ariels stable performance include simultaneous multi-wavelength observations, continuous monitoring of transit events, and a payload design that mitigates or allows for the removal of systematics in data analysis.

The most significant disturbances of astrophysical and instrumental origin are listed in Table 1, along with the strategies employed to mitigate their impact on detection and photometric stability.

Table 1. Summary of noise sources and systematic errors.

Type of uncertainty	Source	Mitigation Strategy
Detector noise	Dark current noise	Choice of low-noise detectors
	Readout noise	
	Gain stability	Calibration, post- processing data analysis, choice of stable detectors, thermal stability of both cold and warm electronics
	Persistence	Post-processing decorrelation. Continuously staring at a target for the whole duration of the observation.
Thermal noise	Emission from telescope, common optics and all optical elements	Negligible due to surface emissivity properties and in-flight temperatures of the payload.
	Temperature fluctuations in time	Negligible impact by design
Astrophysical noise	Photon noise arising from the target	Fundamental noise limit, choice of aperture size (M1 diameter).
	Photon noise arising from local zodiacal light	Negligible over Ariel band
	Stellar variability with time	Multi-wavelength stellar monitoring, post-processing decorrelation
Pointing jitter	RPE and PDE effects on the position, Spectral Energy Distribution, and detector intra/inter pixel response	Small RPE and PDE, Nyquist sampling, post-processing decorrelation
	Slit losses	Spectrometer input slit sufficiently large

Details of the predicted noise budget and the performance of the mission can be found in Pascale et al. [3].

### 3. PAYLOAD LEVEL OPTICAL DESIGN

The optical system can be broken down into a number of separate modules, namely the telescope, the common optics, AIRS and the FGS.

The telescope is a Cassegrain design (parabolic primary M1 and hyperbolic secondary M2) with a third mirror M3 used to recollimate the beam. A fourth mirror M4 directs the collimated beam onto the optical bench. The telescope optical design is described in more detail in [4]. Figure 3-1 shows the telescope optical layout also including the first common optics mirror, M5. M4 is positioned to put the output collimated beam 275 mm from the optical surface of the primary mirror (in the operating case at a temperature of 60K in zero-g conditions).

The entrance baffle, a cut cylinder extending the length of the Telescope Metering Structure, limits M1’s view of the sky. In combination with placing a stop close to the first optical surface (M1), this provides the first line of defense to block out-of-field light. An additional baffle is positioned over the ‘top’ of M2 (as viewed in Figure 3-1) to block any direct view of the sky from M2 past the end of the entrance baffle. These are both in place as good stray-light design practice but are also useful from a thermal control point of view.

Note that a tilt of the telescope with respect to the mounting plane of the PLM to the SVM has been introduced in order to allow sufficient design room for the mounting bi-pods. This means that Yopt and Zopt axes are not coincident with the respective mechanical axes, but are offset by 5°.

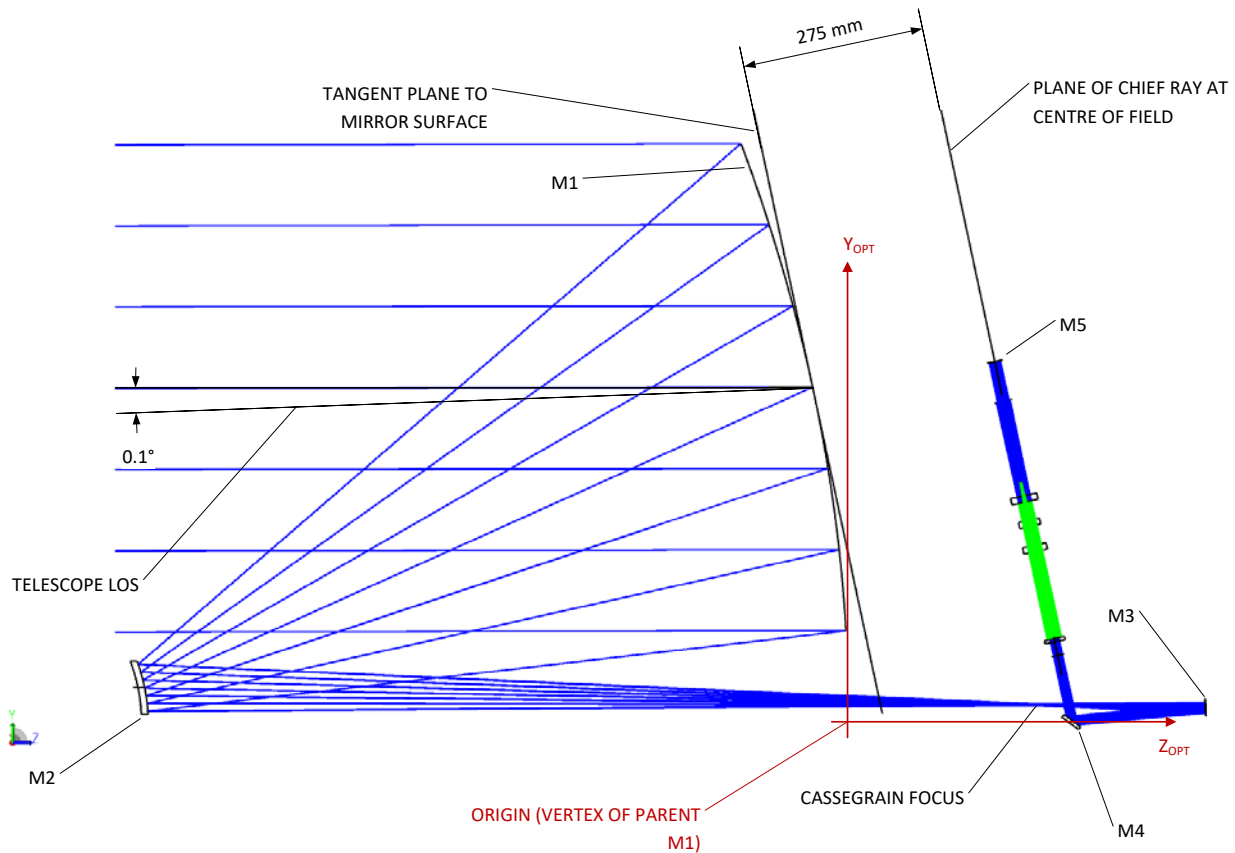


Figure 3-1: Scale drawing of the telescope – view in  $Y_{OPT}$ - $Z_{OPT}$  plane. The  $0.1^\circ$  offset is exaggerated for clarity. Cold case.

M2 has a refocus mechanism with three degrees of freedom as a baseline (focus and tip/tilt). The purpose is to correct for one-off movements due to launch loads and cool-down and potentially to make occasional adjustments (for example to compensate for any long term drifts in structural stability). To determine the optical focus position a two-step process is used to close the loop. First, a suitably bright star is observed and the peak amplitude of the PSF is monitored on FGS-1 and FGS-2 as M2 is moved. Although affected by a large WFE relative to their central wavelengths, the PSF in these bands is expected to have a well-defined central lobe. Once the optimal focus is found in this way, the telescope attitude can be commanded to place the same star onto the slit of AIRS (AIRS-1). We can then move M2 and monitor the peak amplitude of the spectra in all spectroscopic channels. The optimal focus position is obtained when the peak signal is maximum as this condition maximises the SNR of the science detection. There is a chance that the M2M may be used to deliberately “defocus” the telescope in case the as-built PSF is more compact than expected in order to avoid saturation of the detectors on the brightest targets.

As M2 is moved, also the position of the star (and its spectrum) moves on AIRS and FGS. Because FGS closes the AOCS loop, this ensures that the star is kept onto the slit at all times during focusing operation. Scanning the spacecraft such that the source is moved orthogonally to the slit will allow to identify when the source is crossing the slit centre. When that occurs, the position of the same source on the FGS-1 and -2 focal planes is recorded as being coincident with the bore-sight of AIRS.

After the Cassegrain focus, the beam is recollimated by M3. The baseline design has M3 as an off-axis-paraboloid on the same symmetry axis as that of M1,M2. This results in a recollimated beam, i.e. M1,M2,M3 form an afocal telescope, with beam of size 20 mm x 13.3 mm. Then follows the fold mirror M4, used to direct the beam onto the optical bench.

Figure 3-2 shows the telescope and common optics layout as viewed from the rear of the M1. Details of optical design parameters and requirement of the telescope are presented in Pace et al [4]

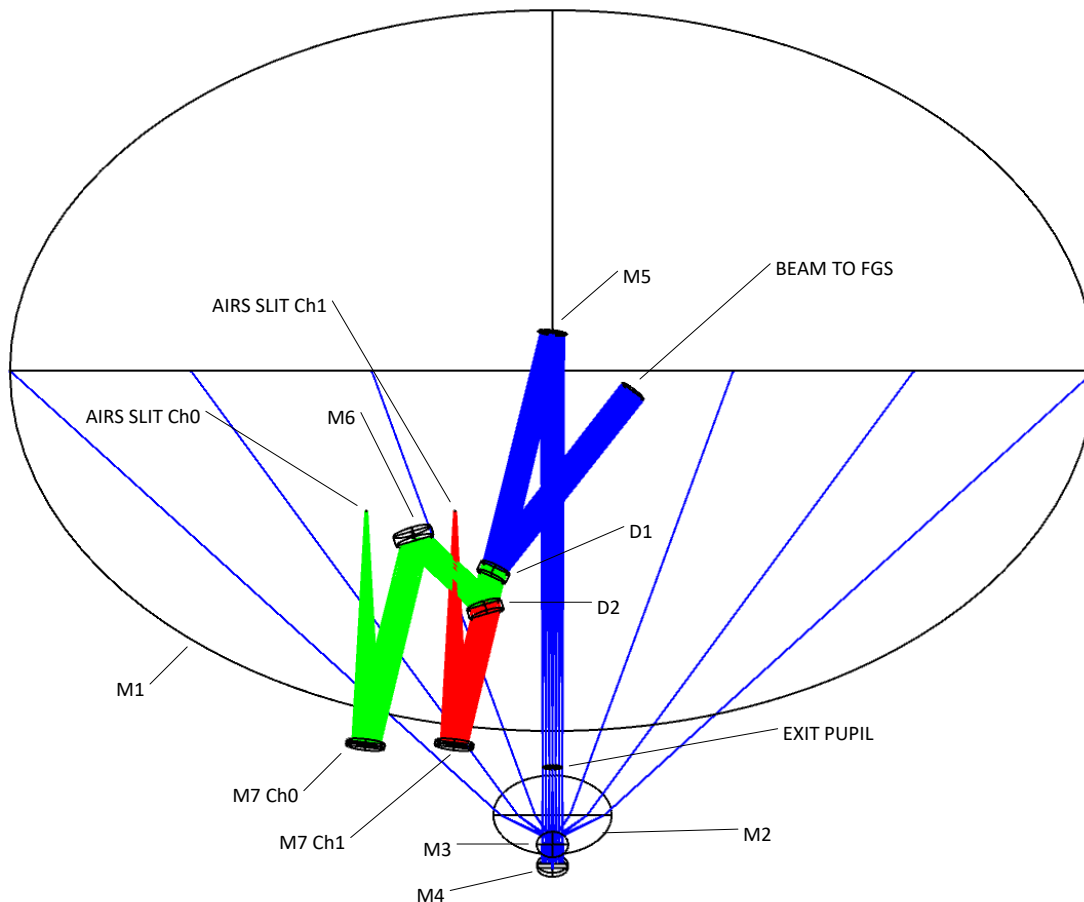


Figure 3-2: Scale drawing of the telescope and common optics – view in  $X_{OPT}$ - $Y_{OPT}$  plane

The beam from M4 travels to another fold mirror M5 which deflects the beam back at a modest angle to allow accommodation of the dichroic beamsplitters (D1 & D2) and AIRS input optics (M6, M7-0, M-1). The beam from M4 runs parallel to the sides of the optical bench (vertically, parallel to the plane of the mounting interface for the instruments) and the elliptical pupil on the optical bench is orientated such that the major axis is parallel to the plane of the bench.

The first dichroic, D1, is used to split light between the FGS and AIRS instruments, with a transition at 1.95  $\mu\text{m}$ . The dichroics are laid out to minimise angle of incidence, which is always kept below  $30^\circ$ . The short wave beam from D1 passes to the FGS, which provides two guiding channels along with a visible photometric band and a low resolution ( $R > 15$ ) NIR spectrometer.

The long-wave beam from D1 is further split by D2 into two wavebands, of one octave each (1.95  $\mu\text{m}$  – 3.9  $\mu\text{m}$  and 3.9  $\mu\text{m}$  – 7.8  $\mu\text{m}$ ). Each of these two paths is focused onto the spectrometer entrance slit by an identical off-axis parabola M7, the function of which is to deliver the correct input f-numbers. The mirror focal length is chosen to deliver a beam with  $f/12$  (major pupil axis) and  $f/18$  (minor pupil axis). An additional fold mirror M6 is used to space the centres of the AIRS input slits apart by 108.4 mm – the agreed interface with AIRS. The two spectrometers have independent optical channels. Channel 0 gives  $R=100$  over the shorter waveband (1.95 – 3.9  $\mu\text{m}$ ) while channel 1 gives  $R=30$  over the longer waveband (3.9 – 7.8  $\mu\text{m}$ ).

#### 4. PAYLOAD LEVEL MECHANICAL DESIGN

The main mechanical design drivers for the structural elements of the Payload Module are to support the optical elements and science subsystems in a sufficiently stiff and strong manner to survive the launch and operational environments, whilst also allowing for the contraction of the Payload as the operational temperature is reached.

The optical elements M1 to M4 are mounted to the structural components of the Telescope Assembly (TA). These structural components are manufactured from grades of aluminium alloy similar to the mirrors themselves, so that the telescope remains aligned as it cools to operational temperature.

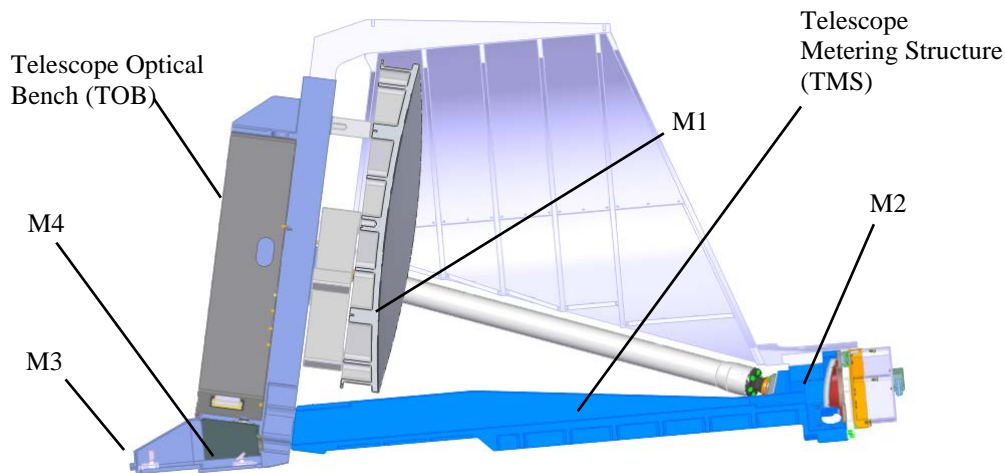


Figure 4-1 Telescope Assembly Structural and Optical Elements

The Baffle Assembly surrounding the M1 mirror and covering M2 is not structurally intended as the primary load paths for the telescope assembly. It is attached to the TOB and to the front end of the TMS. It is also manufactured from aluminium alloy to minimise the stresses induced from the cooldown of the TA structure and to minimize the thermal gradients so as to allow its use as additional radiator area for cooling the PLM.

One consequence of the all-aluminium construction of the TA coupled with the cold temperatures required for operation is the large contraction of the TA relative to the Spacecraft Module. The TA must also be thermally isolated from the Spacecraft Module for those temperatures to be achieved. The TA supporting structure must therefore have low thermal conductivity and low stiffness, so that the TA is not significantly distorted by the differential contraction. However, the stiffness must be sufficiently high to avoid the risk of modal coupling between the Payload and Spacecraft during launch, and to avoid micro-vibration resonances in operation. These requirements are met by the Bipods; six struts that connect the TA to the Spacecraft Module, at the Payload Interface Plate (PIP).

To achieve the required operational temperatures, the TA must also be shielded from the thermal radiation emitted and reflected from the Spacecraft Module. The V-Groove assembly performs this function. The mechanical design drivers for the V-Grooves are similar to those of the TA and Bipods; flexibility to avoid excessive stresses due to thermal contraction, whilst achieving sufficient stiffness and strength to survive the launch environment, within the allocated mass budget. The V-Grooves are each at different temperatures in operation, hence their support structures must also be thermally isolating.

There are no structural connections between the V-Grooves and the rest of the Payload, except via the PIP (to minimise the effects of any structural deformations of the V-Grooves on the Telescope). The V-Groove panels themselves are constructed from aluminium alloy honeycomb with reflective aluminium alloy face skins (except the upper surface facing deep space which is black painted open honeycomb). The support struts between them are made from glass fibre reinforced plastic (GFRP), for thermal isolation. The limited accommodation available for the V-Grooves (between the TA and the PIP) restricts the length of the central V-Groove supports, and it was necessary to recess these supports into the PIP to provide adequate length to achieve the thermal isolation and flexibility required.

## Payload Accommodation

The Payload has been designed to fit within the Shadow Cone Volume – this is a volume defined by the dimensions of the Spacecraft Module and the permitted orientations of the Spacecraft with respect to the Sun, such that the Payload is always in shadow during all operational phases of the mission. The geometry of the V-Grooves is designed to exactly match the edge of this shadow cone in order to ensure that there is never a direct view of any of the stages of the panels to either the sun or to the PIP.

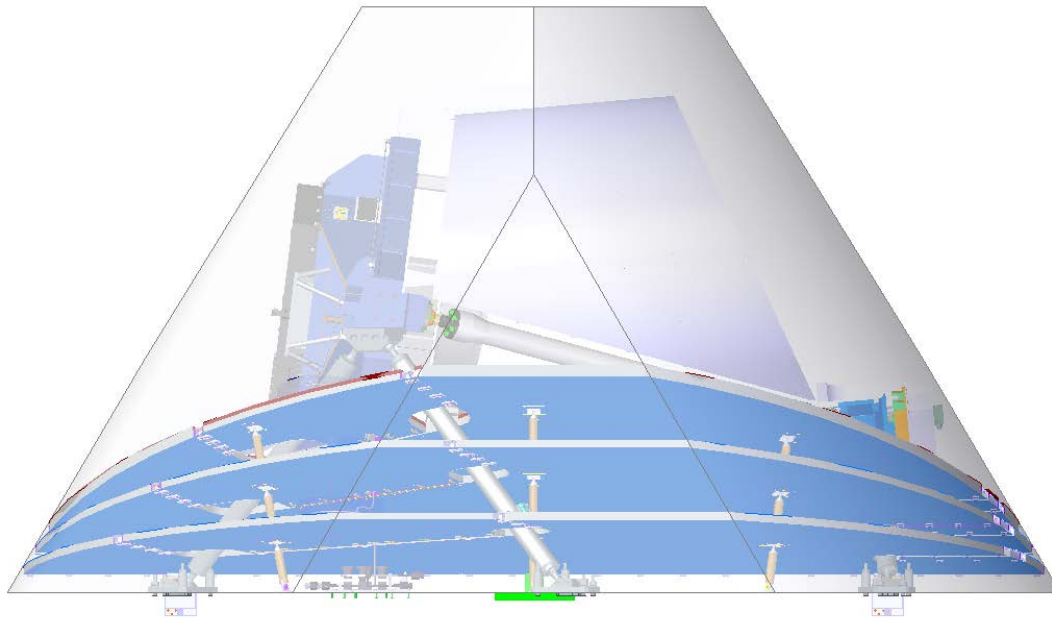


Figure 4-2 PLM within Shadow Cone

## Bipod structural design

The Bipod struts which support the mass of the payload module from the SVM consist of hollow CFRP (carbon fibre reinforced polymer) cylinders; CFRP was selected to provide the optimum balance of low thermal conduction and good structural properties for the temperature range applicable (isolating 50K PLM from 273K PIP). To increase their thermal performance by reducing radiative heat exchange within the tubes, the inner volume of the cylinders are filled with low thermally conductive rigid foam. Titanium alloy flexures at the top and bottom of each Bipods strut provide sufficient strength to survive the mechanical environmental loads whilst allowing sufficient flexibility to accommodate the thermal contraction of the Telescope Assembly structure, without causing unacceptable distortion. The struts are equipped with strain gauges close to the lower flexures to monitor the strains induced during integration activities and during vibration testing. These gauges will remain in place but are not used in flight. The conducted and radiative heat leaks of the bipod struts are intercepted on the three V-Groove stages by means of thermal straps which connect to Invar rings bonded to the CFRP tubes.

The interfaces to the Telescope Assembly consist of aluminium alloy components, to match the material of the TA. Shoulder bolts (for the front Bipods) and dowels (for the rear Bipods) have been included in the bolted joints to ensure slippage does not occur and for alignment repeatability. Differential contraction between the Titanium flexure and the aluminium interface components is provided for via an Invar spacer.

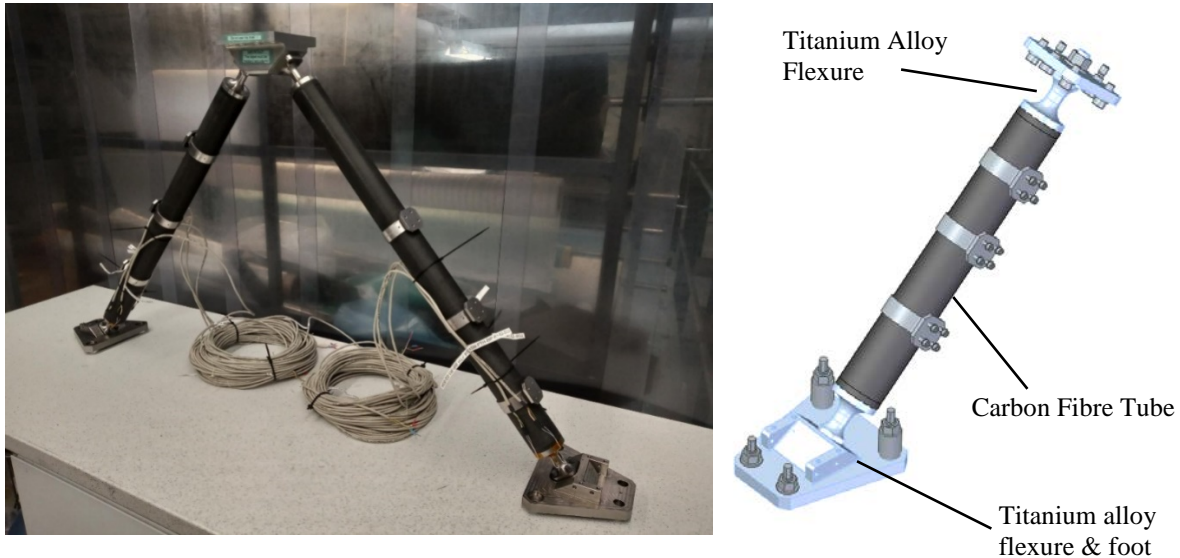


Figure 4-3: Photograph of SM rear bi-pod set (left); diagram of Single front Bipod strut (right)

### Payload ancillary hardware design

The PLM ancillary equipment includes: purge hardware, sub-system interface fixings and closeouts, instrument cavity optical baffles (for control of potential scattered straylight paths), and harness support components.

The payload requires a supply of dry, clean, inert gas to be provided as a purge supply before flight to maintain the cleanliness of the sensitive optical elements of the payload within the instrument cavity and the instruments and to keep the M2 Mechanism (M2M) (in particular the actuator gearboxes) in low humidity environment.

The purge system for the PLM connects the purge inlet from the spacecraft (or GSE during payload ground activities) to two independent Swagelok bulkhead connectors – one on the PLM optical bench (+Z wall of the instrument cavity), and one on the M2M at the front of the PLM. The purge pipe is made in PTFE (doped for electrical surface dissipation) for the section which runs up the bipod strut in order to minimize the conducted parasitic thermal loads, then in stainless steel for the isothermal sections which run on the TOB and TMS.

### Structural modelling

Details of the structural design and modelling challenges of the payload can be found in Bruzzi et al [5].

## 5. PAYLOAD LEVEL THERMAL DESIGN

The function of the thermal design of the cold PLM is to shield the scientific instrumentation (the Ariel instruments and the Telescope Assembly) from the warm section of the S/C and to provide it with the required cooling and thermal stability at temperatures < 60K.

Passive cooling is achieved by a high efficiency thermal shielding system (Figure 5-1) based on a multiple radiators configuration that, in the L2 environment, can provide stable temperature stages down to the 50 K range. At 1.5 million km from the Earth in the anti-Sun direction, the L2 orbit allows to maintain broadly the same spacecraft attitude relative to the Sun-Earth system, while scanning the whole sky during the mission. Limiting the allowed Solar Aspect Angle (SAA) range, Ariel operates in a very stable thermal environment keeping always in the shade the coldest section of the PLM from the Sun/Earth/Moon illumination. For this reason, the SAA allowed during nominal observations is limited to  $\pm 5^\circ$  around the spacecraft Y-axis and to  $\pm 25^\circ$  around the X-axis. Due to possible contingencies, mainly related to the first phases of the mission, an extra margin of, respectively,  $6^\circ$  and  $5^\circ$ , has been assumed on these values: the thermo-mechanical architecture of the PLM has been designed within a total envelope of  $\pm 11^\circ$  around the spacecraft Y-axis and  $\pm 30^\circ$  around the X-axis (Figure 4-2).

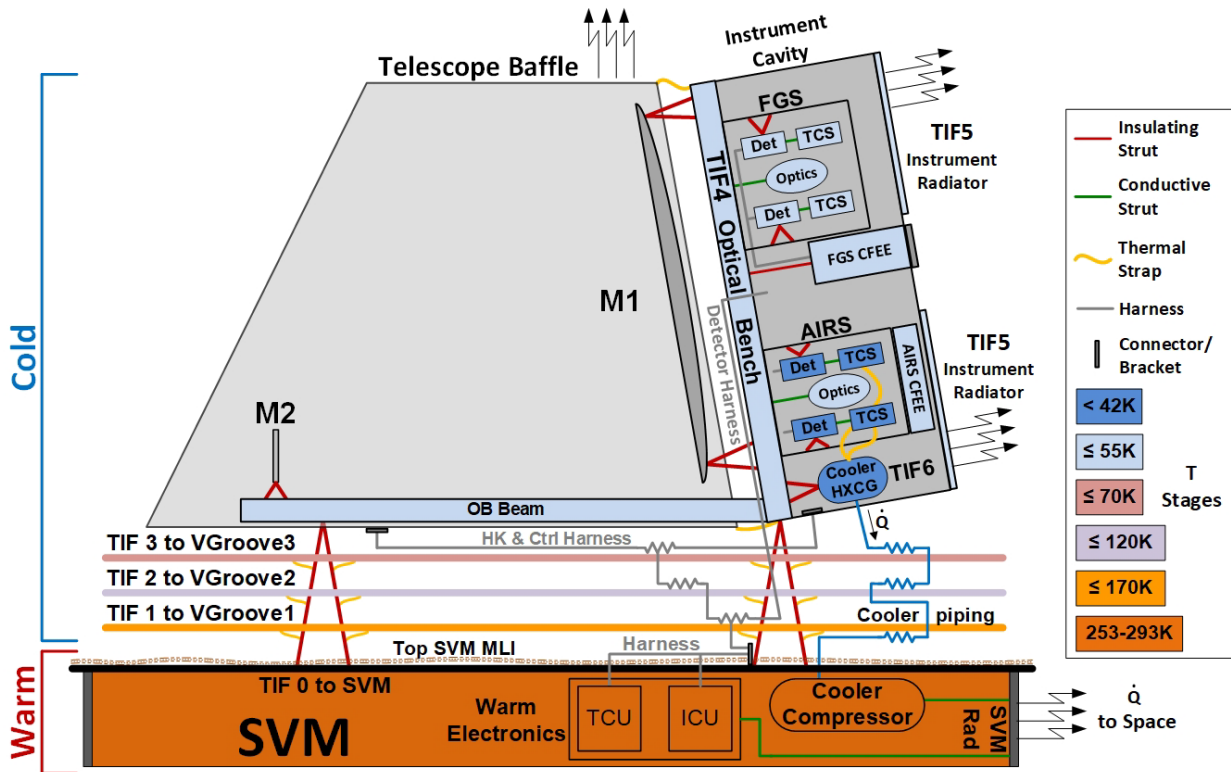


Figure 5-1: PLM thermal Architecture Scheme

The SVM upper platform, the main thermo-mechanical interface of the PLM to the S/C, operates in the range 253 – 293K and is covered with a black Kapton MLI blanket, acting as the first main radiative barrier between the PLM and the warm units in the service module.

The telescope is required to operate at a temperature  $< 70\text{K}$ . The Telescope Assembly (TA), enclosed in the cold environment established by the last V-Groove, acts as an extra passive stage using its large Baffle and Optical Bench (TOB) as radiating surfaces. These radiators, coated by high IR emissivity paints (MAP PUK AQ and Z307), greatly improve the efficiency and the performances of the whole PLM passive cooling. The whole telescope structure and the mirrors reach, at steady state, temperatures in the 50-60K range with only a few degrees' difference between the Hot and Cold case, demonstrating the excellent performances of the passive cooling system in shielding the coldest stages from the warm sections of the S/C. An extra passive cooling area is provided by the Instrument Radiator (see below), the top surface that closes the instrument modules cavity of the TOB.

The modules of the Ariel instruments, the Ariel InfraRed Spectrometer (AIRS) and the Fine Guidance System (FGS), are integrated on the Optical Bench, in the Instrument Cavity, each one including optical units and two detector channels. Cooling of the AIRS and FGS module boxes with the internal optical units is achieved by thermal coupling to the TOB. The operating temperature of the FGS and AIRS detectors is achieved following a diverse approach, according to the different temperature requirements of each frequency band. The detectors of the FGS, mounted on the instrument box, are passively cooled to  $T \leq 70\text{K}$  by their coupling to the Telescope Optical Bench through the module structure. The AIRS detectors must be operated at a colder temperature, below 42K, to minimise detector noise. Maintaining this temperature, with dissipation and parasitic loads of tens of mW, requires an active cooling system. The cryocooler-selected baseline relies on the Planck mission and EChO project study heritage: a JT cold end fed by a mechanical compressor using Neon gas isenthalpic expansion to achieve the required low temperature and heat lift (see below for details).

The FGS modules' Cold Front End Electronics (CFEE) design is based on SIDECAR units provided by NASA JPL. Due to cryogenic qualification issues inherited from previous projects, the FGS SIDECAR thermo-mechanical packaging requires a PLM thermal design capable of maintaining the SIDECARs box at all times above a safe temperature of 130K.

In order to ensure electrical performance of the detector system, the cryo-harness connecting the electronics to the detectors cannot be longer than few tens of cm. This means that the FGS CFEE box shall also be integrated in close proximity of the FGS-SCAs. Therefore a separate module housing the SIDE CARs and with its own small radiator, maintained at ~133K in all operational conditions, is mounted on isolating GFRP struts on the optics bench just outside of the optical cavity. In all Operating Modes with the PLM at cryogenic temperature and the FGS CFEE in an OFF state, the automatic activation of a survival heating line by the S/C is required to ensure that the hardware is continuously maintained above the qualification limit.

The two FGS channels are integrated in a single Module Box and work in the same temperature range, with the optical units and the detectors at a temperature, respectively,  $\leq 60\text{K}$  and  $\leq 70\text{K}$ . The whole module box, including the detector focal planes, is passively cooled by a contact conductive interface to the Telescope Optical Bench stage (TIF4 in Figure 5-1) that operates inside the cold environment set by the third V-Groove. Both FGS detectors are thermally decoupled from the Module Box to allow for a fine thermal control stage that will keep them at a constant set point for approximately the whole duration of the mission in order to stabilize the thermal impact on detector system gain variations.

As already mentioned, the AIRS detectors technology baseline requires an operating temperature  $\leq 42\text{K}$  with a goal of 36K, to achieve the required sensitivity. This temperature is reached by connecting the AIRS SCAs by means of copper thermal straps to the ACS (a Ne JT cooler fed by a mechanical compressor), capable of producing a heat lift  $> 90\text{ mW}$ . In order to provide the required cooling to the AIRS detectors, the ACS cold end heat exchanger is located in close proximity to the FPAs, to minimize the distance and the thermal strap length, and supported on the Optical Bench by an insulating GFRP strut.

The AIRS module box, including the optical system, is thermally coupled to the TOB and shall operate at a temperature lower than 60K. The FPAs, mounted on the AIRS module, need to be insulated from the box, to limit the heat leak to the JT cold tip and to allow for a fine thermal control operated, by the AIRS DCU via a built-in control loop, under the responsibility of the module development team. Each AIRS discrete CFEE unit is mounted directly on the relative focal plane channel but is thermally coupled to the module box, rejecting the heat load directly to the TOB. The AIRS CFEEs operate at a temperature few degrees higher than the OB.

The warm electronics and cooler compressor are located in the SVM. Cooler piping, detectors and thermal/M2M control harness from SVM to cold PLM shall be thermally linked to all passive stages (VG1, VG2, VG3) to minimize parasitic leaks on the instrument cooling stages, with the exception of the FGS detectors control harness (from the FCU to the SCE) that is thermally coupled to the VG1 only. This solution is adopted to help the thermal control of the channel CFEEs. The cables can operate as significant thermal conductors, so their heat leak into the CFEE is used as an extra passive load to help maintaining the electronics temperature above the safety limit.

### **Design of V-Groove passive radiator system**

The V-Grooves (VGR) are high efficiency, passive radiant coolers, providing the first stage of the PLM cooling system. The Planck mission demonstrated their efficiency as passive cooling systems. Parasitic heat from warmer sections of the S/C is intercepted by the VGRs and radiated to space after multiple reflections between the adjacent shields. To achieve this, VGRs surfaces must have a very low emittance coating, a high reflection/mirroring material needed to reflect heat radiation. Only the upper surface of the last VGR (VG3), exposed to the sky, is black coated with a high emissivity material (thermal paint applied to open honeycomb core) to maximize the radiative coupling, and so heat rejection to deep space.

The VGRs consist of a set of three specular shields, composed of six half circles arranged in a “V-shaped” configuration, angled along the diameter parallel to the S/C X axis. A constant angle of  $7^\circ$  has been chosen as the optimum inclination between V-Grooves, resulting in a set of  $7^\circ$ - $14^\circ$ - $21^\circ$  for the three shields. The V-Grooves are mechanically designed as a 20 mm (17 mm in the removable sections) thick sandwich, consisting of 0.3 mm thick aluminum alloy (MIRO 27) and an aluminum honeycomb cell structure.

This thermo-mechanical configuration has several advantages: it achieves great thermal shielding in a relatively compact volume and reduced mass; it is a simple construction, totally passive, and has a high reliability; and there is no need for deployment, vibration free.

The VGRs are thermally linked to the PLM three bipods via flexible cold links made of pyrolytic graphite sheets (PGS), but are mechanically supported separately by the SVM by eight GRP struts.

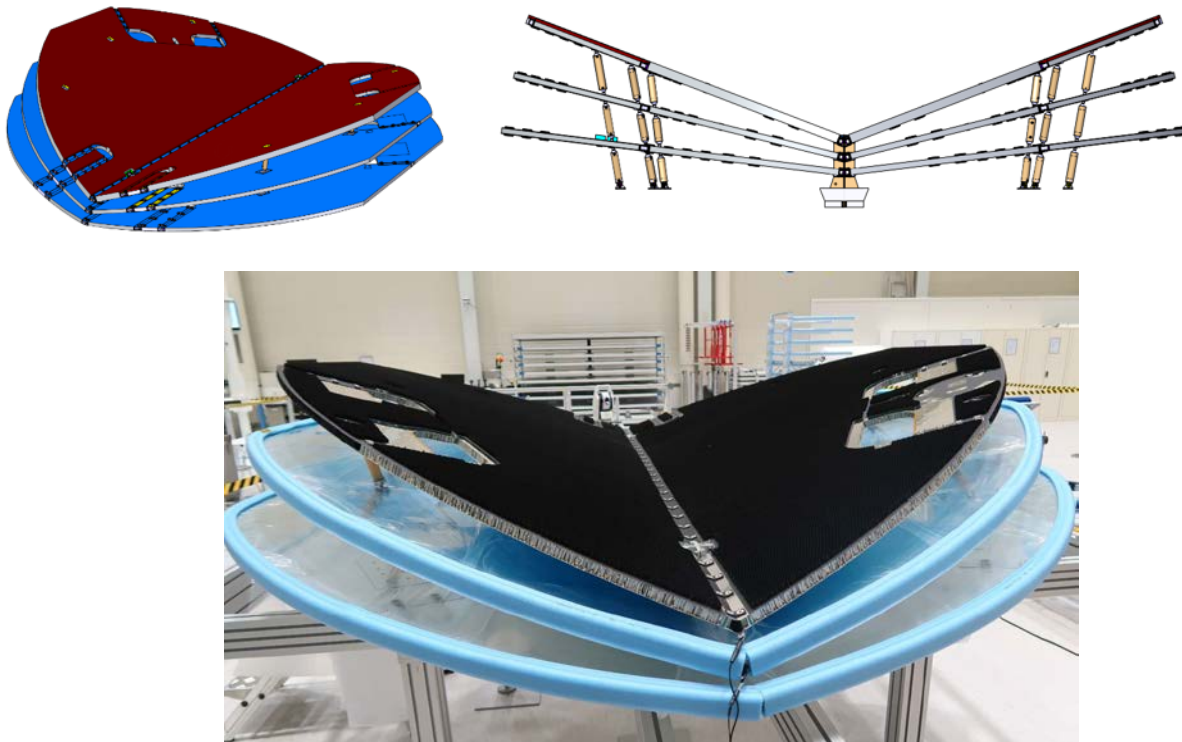


Figure 5-2: V-Groove design (upper), V-Groove STMs with protective covers of lower VGs (lower)

### Design of Instrument Radiator (IR) system

The instrument radiator, shown in Figure 5-3, provides a means of passive cooling for the instrument cavity while creating light tight enclosure required for the detector systems. The main radiator body is made of two integrally milled halves with an open honeycombe pattern machined into the exterior face to maximise the effective emmissivity. The radiator has an opening for integration purposes during payload AIT, which is covered by the third main part called hatch cover.

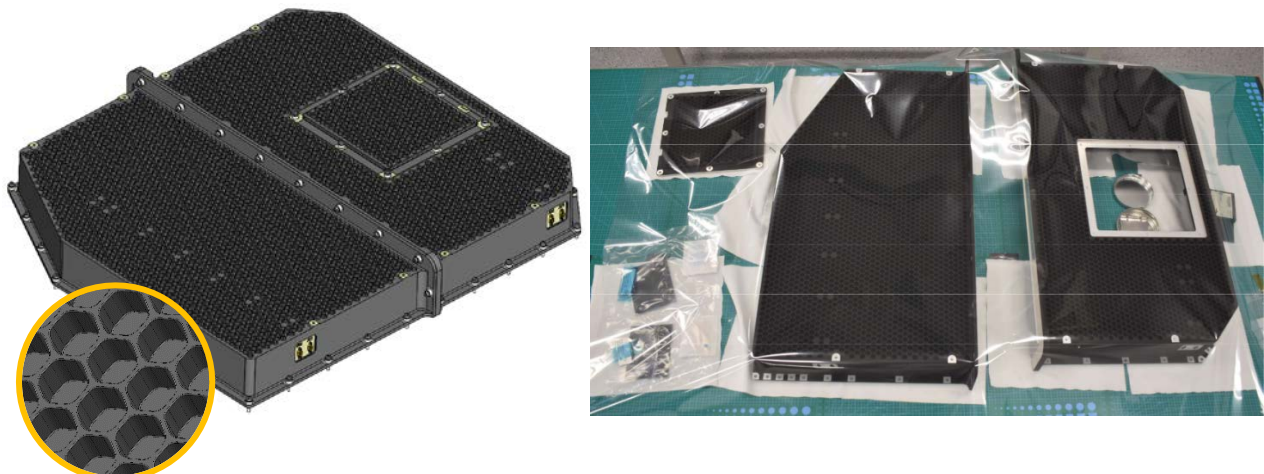


Figure 5-3: Design of the Instrument Radiator and photo of the STM hardware.

All the three main parts are made of aluminium alloy AA6082 T651 and are coated by high emissivity black thermo-optical coating MAP AQ PUK except for mechanical interfaces, that are conversion coated using Surtec 650. Efficiency of main radiative interface parallel to mounting plane is enhanced by open honeycomb structure with 8mm diameter and 8mm deep cells having 1mm wall thickness. The 3.8mm thick aluminium walls of IR provide decent protection against radiation for instruments located in instrument cavity.

A large stiffener is added in the middle of radiator (at the interface of PZ and MZ halves), which is critical to achieve sufficient stiffness within the allocated mass budget. Light tightness of instrument cavity is ensured by a lip on the radiator around TOB interface protruding 2mm below the mounting plane.

## 6. PAYLOAD LEVEL ELECTRICAL AND ELECTRONICS DESIGN

The detailed electrical and electronics design of the payload, including the design evolution through the payload PDR period is discussed in Focardi et al [6].

### Power budget summary

The summary of the power budget for the payload is shown in Table 6-1 below. The overall payload power is compliant to all of the relevant requirements with margins that are commensurate with the state of the design.

Table 6-1: Power Budget Overview by mode / configuration, all values are CBE (W)

Subsystem	Transition / Decont	Safe Mode	ACS Gas Cleaning	Science Modes
ICU	14.92	0	0	20.53
ADCU	0	0	0	13
ICU + ADCU	14.92	0	0	33.53
TCU	11.11	0	0	26.49
FCU	0	0	0	29.98
ACS	10.07	0	35.07	73.7
Total	36.1	0	35.07	163.70
Total with 20% <u>System Margin</u>	43.32	0	42.08	196.44
PLM Decontamination Heaters	182.4	0	0	0
PLM Survival Heaters	2	2	2	0
Power margin (%)	24.8%	0%	36.2%	12.9%

### Data budget summary

The data volume budget and compliance for the payload in Gbits/wk is given in Table 6-2. Both the data volume and the peak data rate budgets are compliant to the requirements with ample margins.

Table 6-2: Data Volume budget compared to allocations in Payload Requirements Document

Name	Description	Allocation	Current Best Estimate
<b>Nominal Science rates / Week</b>		<b>(Gbit/wk)</b>	<b>(Gbit/wk)</b>
FGS	Science data + AOCS data stream + internal HK	64.0	60.8
ICU	Science data + internal HK + A-DCU HK	126.8	120.9

TCU	Thermal monitoring + M2M TM + others	2.3	0.7
CCE	Cooler HK & TM	0.8	0.6
Margin	System Margin (20%)	47.2	53.1
<b>Total</b>	<b>Payload Total (incl. margin)</b>	<b>236.0</b>	<b>219.5</b>
<b>Commissioning data rates / Day</b>		<b>(Gbit/day)</b>	<b>(Gbit/day)</b>
FGS	Science data + AOCS data stream + internal HK		9.1
ICU	Science data + internal HK + A-DCU HK + TCU HK		18.2
CCE	Cooler HK & TM		0.1
Margin	System Margin (20%)	20.0	5.4
<b>Total</b>	<b>Payload Total (incl. margin)</b>	<b>100.0</b>	<b>32.8</b>

## 7. PAYLOAD INSTRUMENT AND MAJOR SUBSYSTEMS DESIGN SUMMARIES

The design of the Telescope Assembly (TA) for the payload is detailed in Pace et al. [4]. A summary of the optical design is given in section 3 above and some images showing the mechanical design can be found in section 4.

The design of the AIRS instrument is given in detail in Martinac et al. [7].

The design of the FGS instrument can be found in Skup et al. [8].

Details of the hardware design of the ICU can be found in Noce et al. [9], while the design of the application software which controls the unit and handles the spectrometer data can be found in Ligori et al. [10].

### Active Cooler System (ACS) design

The Active Cooling System is a closed cycle Joule-Thomson (JT) mechanical cryocooler using Neon as the working fluid. A schematic of the ACS is shown in Figure 7-1.

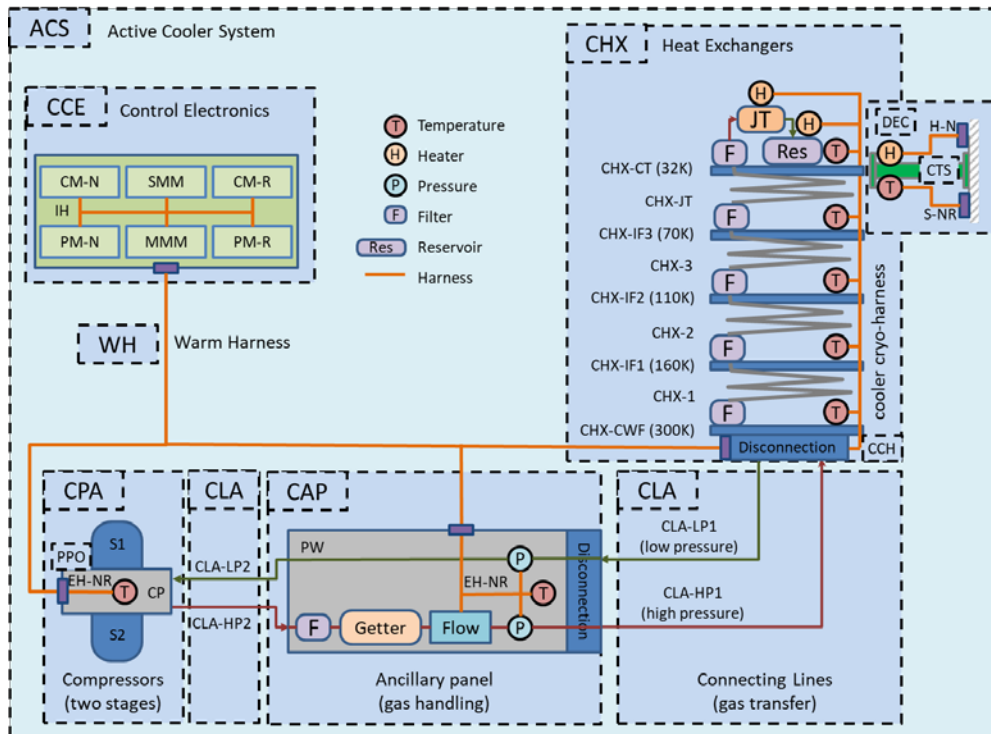


Figure 7-1: JT Cooler Schematic

The ACS provides active cooling at the cold tip thermal interface by performing a Joule-Thomson expansion of the working fluid across a restriction, in this case an orifice. The cooler is operated sub-critical, collecting the liquid produced after expansion in a reservoir such that the heat exchanger return-line pressure above this reservoir determines the temperature. The cooling power achieved depends upon the fluid mass-flow through the orifice as well as the initial and final states of the fluid before and after the expansion process. In general greatest cooling occurs when the fluid is initially pre-cooled well below its inversion temperature, with its initial pressure close to the inversion curve boundary and its final pressure much lower.

The cooler is required to provide 88mW (including margins) of cooling at a temperature of  $\leq 35.0$  K in order for the AIRS detectors to operate at  $< 42$  K. Neon is selected as the working fluid because its boiling point (27.05 K at 1atm) is well matched to the temperature requirement. In nominal operation the return line pressure is designed to be  $\sim 3.5$ bar which gives a cold tip temperature of  $\sim 32$  K, and the inlet line pressure is designed to be  $\sim 20$ bar, which is very much lower than the inversion curve boundary ( $\sim 300$ bar at 100K), but is accessible for reciprocating compressors.

The compressors (CPA) circulate the Ne gas around the system by a set of reciprocating linear motor compression stages, with an arrangement of reed valves and buffer volumes, to produce a DC flow through the Joule-Thomson orifice whilst maintaining the pressure ratio across it. Two compression stages in series (CPA-S1 and CPA-S2) are needed in order to produce the required high and low pressures.

The gas must be pre-cooled prior to the Joule-Thomson expansion taking place, there are three pre-cooling stages available from the spacecraft V-groove radiators and, to reduce the heat rejected at these pre-cooling interfaces (CHX-IFn), counter-flow heat exchangers (CHX-n) are used between them.

The ancillary panel (CAP) carries gas handling and measuring equipment, as well as particulate filters and a reactive getter to ensure gas cleanliness, which is critical to the long-term operation of the cooler. The disconnection plates and connecting pipework (CLA) allow the system to be broken into several pieces to aid integration. This allows the heat exchanger assembly to be delivered and integrated with an instrument separately from the CPA and CAP, with a final purge and gas fill procedure being carried out after installation of the CLA to join the CPA/CAP to the CHX.

The cooler is controlled by a set of drive electronics (CCE) which perform all commanding and controlling functions, including active exported micro-vibration reduction, as well as providing the electrical input power for the compressors and returning the cooler housekeeping data. The overall high-level block diagram of the Ariel CCE is shown in Figure 7-3.

The development model / qualification model hardware for the various cooler components are pictured in Figure 7-2.

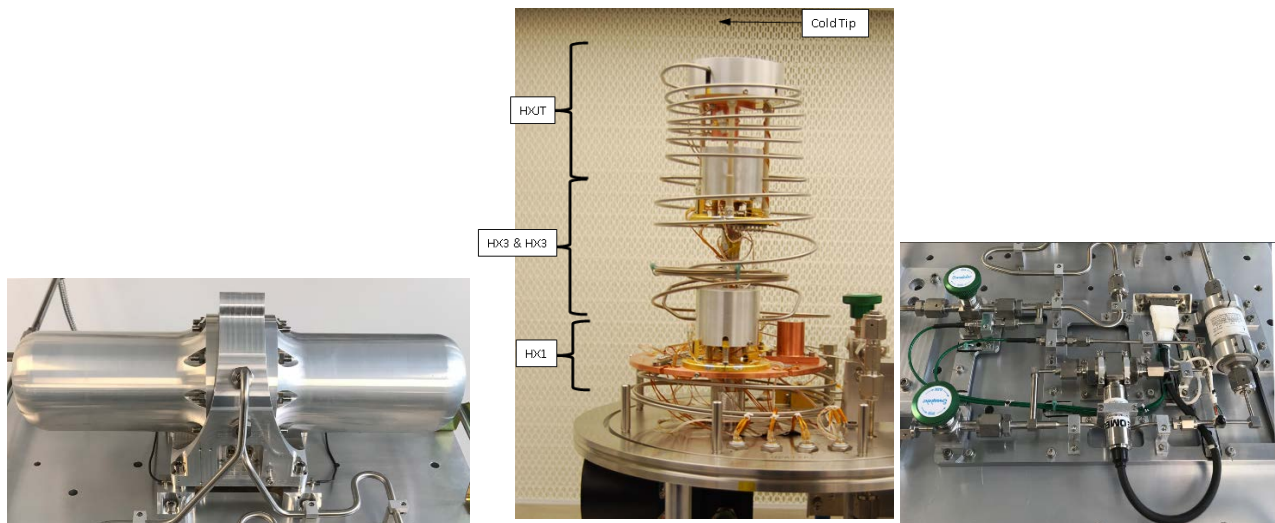


Figure 7-2: (left) ACS Demonstration Model Compressor Assembly (CPA), (centre) ACS Demonstration Model Heat Exchanger Assembly (CHX) configured for test with a COTS cryocooler, (right) ACS DM Cooler Ancillary Panel (CAP).

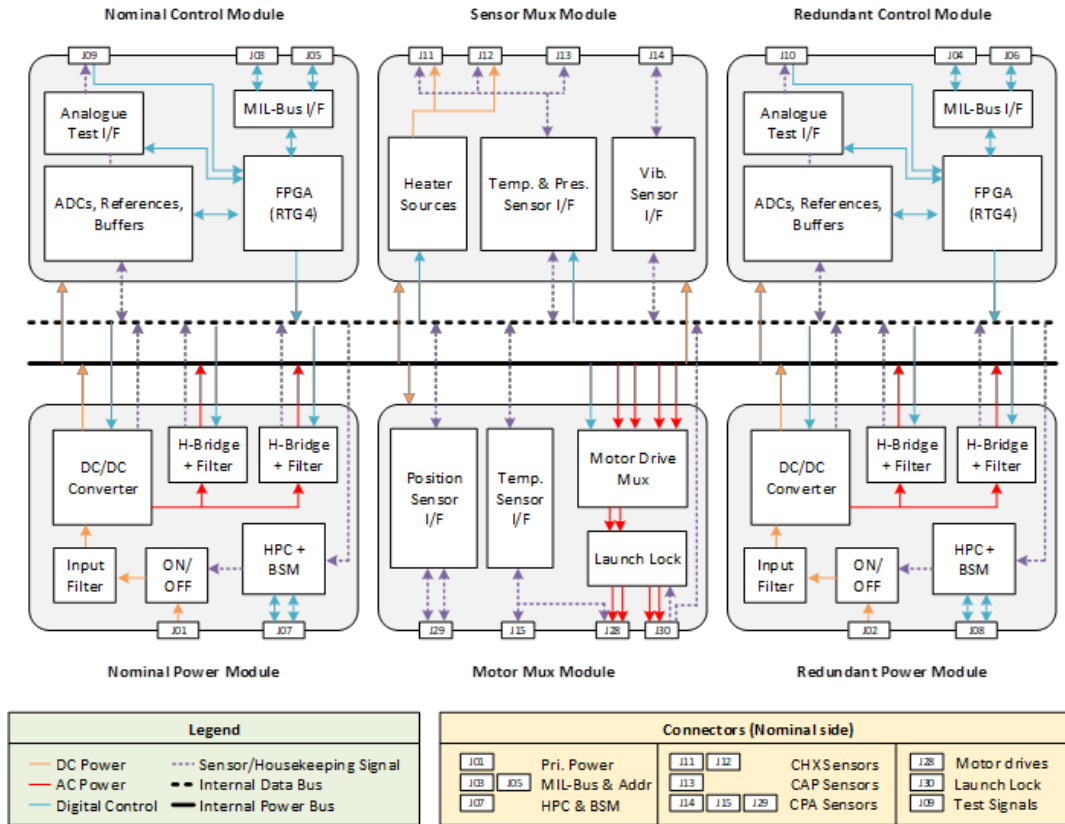


Figure 7-3: Overall CCE Block Diagram

### Telescope Control Unit (TCU) design

The Telescope Control Unit (TCU) has two main tasks; measuring the temperature of the Payload Module, and driving the M2 Mechanism. For this purpose, it will be composed by three separated boards: a Control and Thermal Sensing (CTS) board, an M2 Mechanism Driver (M2MD) board and a Power Supply Unit (PSU).

The TCU design is based on a cold redundancy philosophy; all subsystems and sensors have a redundant counterpart, where nominal elements will be connected to nominal ones, and redundant elements will be connected only to redundant ones. No nominal board will be able to read or control a redundant sensor/actuator, since they will be electrically isolated. However, the interfaces for the Nominal and Redundant TCU to connect with the ICU will be doubled. This allows data link cross-strapping between the TCU and the ICU.

The selection of N or R systems will be performed by the S/C by providing the required power (+28V) to one or the other by means of a dedicated harness. Only one ICU will control the platform selected TCU and share information with it by means of a LVDS SPI bus. Thanks to the mild environment, the system will be managed by a rad-tolerant FPGA with an FSM to switch between states that perform specific tasks.

## 8. PAYLOAD VERIFICATION AND CALIBRATION PLANNING AND DEVELOPMENT STATUS

Following selection of Ariel as the M4 mission for the ESA Cosmic Vision in March 2018, the Payload SRR was successfully concluded in April 2020 (despite the review having to move to remote working at the last minute). The Payload PDR has been conducted and successfully concluded in November 2022.

The planning for the derisking tests, the verification and the calibration of the payload is proceeding in readiness for AIV activities at PL level which will commence in Q3 2024. The overall development approach at top level is illustrated in

Figure 8-1 below. Key activities are the integration and testing of the payload structural model in late 2024, the instrument, telescope and subsystem Engineering Models which are under test throughout 2024 and into early 2025. The payload Engineering Model (EM) then will be assembled and tested in 2025 in advance of the payload CDR. The instrument, telescope and subsystems will commence the manufacture of their flight models (FMs) after the lower level CDRs (iCDRs) which are taking place between early 2024 and mid-2025. The flight model subsystems are then due to arrive at RAL in the UK in mid 2026 for an integration and test campaign that will lead to delivery of the flight model payload in October 2027.

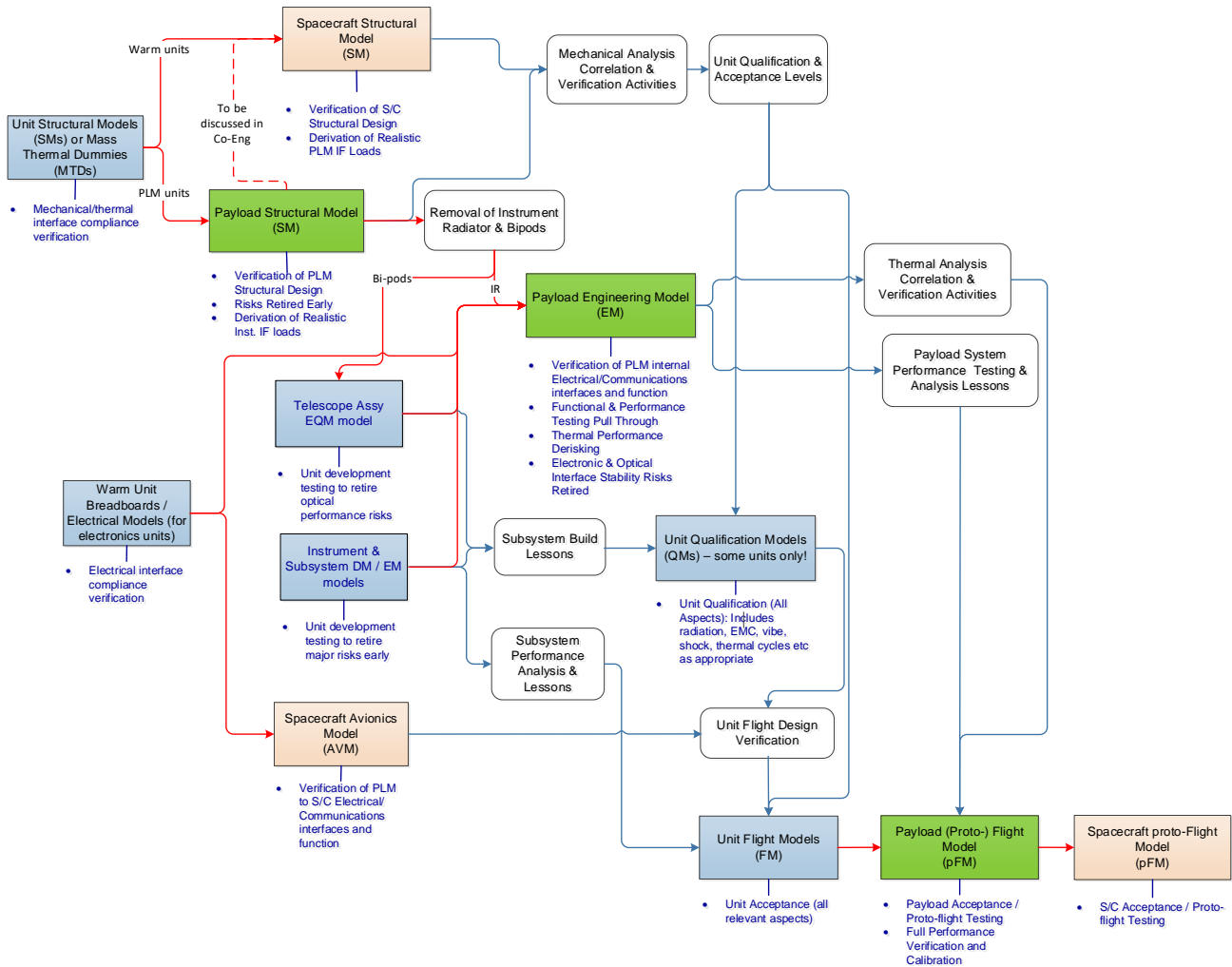


Figure 8-1: Overall verification and derisking flow for payload

## ACKNOWLEDGEMENTS

The Ariel Mission Consortium consists of institutes and industry partners in 17 ESA member states, plus the USA, Canada and Japan. The teams are funded by their respective national funding agencies on numerous grant and contract agreements; some of these use the ESA Prodex system to place the contracts with the industrial and academic partners. The consortium would like to thank all of the funding agencies and respective governments for their support.

## REFERENCES

- [1] Salvignol, J-C. et al., “The Ariel Mission: A mission of the European Space Agency for the characterization of exoplanets”, SPIE Astronomical Telescopes and Instrumentation, Paper 13092-47 (2024).
- [2] Eccleston, P., et al., “Lessons in cat herding – methods used for managing a large international collaborative engineering project, the Ariel Mission Payload”, SPIE Astronomical Telescopes and Instrumentation, Paper 13099-17 (2024).
- [3] Pascale, E., et al., “The Atmospheric Remote-sensing Infrared Exoplanet Large-survey (Ariel) sensitivity and performance”, SPIE Astronomical Telescopes and Instrumentation, Paper 13092-52 (2024).
- [4] Pace, E. et al., “The telescope assembly of the Ariel space mission”, SPIE Astronomical Telescopes and Instrumentation, Paper 13092-49 (2024).
- [5] Bruzzi, D., et al., “Ariel Payload structural architecture: design, analysis and verification challenges”, Proceedings of 17<sup>th</sup> ECSSMET (2023).
- [6] Focardi, M. et al., “The Ariel payload electrical and electronic architecture: a summary of the current design and implementation status”, SPIE Astronomical Telescopes and Instrumentation, Paper 13092-277 (2024).
- [7] Martignac, J. et al., “Ariel IR Spectrometer development status”, SPIE Astronomical Telescopes and Instrumentation, Paper 13092-50 (2024).
- [8] Skup, K., et al., “The Ariel FGS: current design and implementation”, SPIE Astronomical Telescopes and Instrumentation, Paper 13092-51 (2024).
- [9] Noce, V. et al., “The instrument control unit of the AIRS instrument on-board the ARIEL mission: design status after PDR”, SPIE Astronomical Telescopes and Instrumentation, Paper 13092-280 (2024).
- [10] Ligorì, S., et al., “The application software for the instrument control unit of the Ariel mission: report on the development status”, SPIE Astronomical Telescopes and Instrumentation, Paper 13092-281 (2024).